



Dynamics of phase transitions in $\text{Ba}_{1-x}\text{Sr}_x\text{V}_{13}\text{O}_{18}$

Tomohiro Tsukame,¹ Takumi Iwata,¹ Yuki Shiraiishi,¹ Tomomasa Kajita¹ ,¹ and Takuro Katsufuji^{1,2} 

¹*Department of Physics, Waseda University, Tokyo 169-8555, Japan*

²*Kagami Memorial Research Institute for Materials Science and Technology, Waseda University, Tokyo 169-0051, Japan*



(Received 20 April 2022; revised 6 June 2022; accepted 11 July 2022; published 19 July 2022)

We studied the slow dynamics of phase transitions in $\text{Ba}_{1-x}\text{Sr}_x\text{V}_{13}\text{O}_{18}$, which is composed of quasitriangular lattices of V ions and exhibits a phase transition into a V orbital ordered state with V trimerization. We found a clear time dependence of magnetic susceptibility and strain on a phase transition, and the transformation time estimated from the time dependence exhibits a peculiar temperature dependence, consistent with nucleation-growth behavior. Detailed analysis indicates that there is a distribution of the transformation time in $\text{Ba}_{1-x}\text{Sr}_x\text{V}_{13}\text{O}_{18}$, and the formation of twin structures associated with the phase transition may affect the nucleation-growth dynamics and causes such a distribution of the transformation time.

DOI: [10.1103/PhysRevB.106.045124](https://doi.org/10.1103/PhysRevB.106.045124)

I. INTRODUCTION

The slow dynamics of phase transitions has been studied for various types of phase transitions. In particular, the dynamics dominated by nucleation-growth processes are commonly observed, for example, in liquid-crystal or glass-crystal phase transitions [1–9]. In this process, the volume fraction of each phase changes on a characteristic timescale called the transformation time, and its time dependence is theoretically given by the Kolmogorov-Johnson-Mehl-Avrami (KJMA) model [10–13], which takes into account the nucleation of a low-temperature (LT) phase in the high-temperature (HT) phase, the growth of the nuclei, and the impingement of the grown nuclei. The temperature T dependence of the transformation time exhibits a C shape with T on the y axis (or a U shape with T on the x axis), which is dominated by the interfacial energy between the LT phase and the HT phase and the energy barrier between the two phases.

On the other hand, it is rare that phase transitions within crystals exhibit such nucleation-growth behavior, except for martensitic transformations with a large displacement of atoms [14,15]. Recently, however, some organic compounds have been found to exhibit nucleation-growth behavior upon transition between a charge-glass phase and a charge-ordered phase [16–19]. In addition, an inorganic compound, $\text{BaV}_{10}\text{O}_{15}$, with a quasitriangular lattice of V ions, which exhibits an orbital ordering of V ions with V trimerization, has also been found to exhibit nucleation-growth behavior upon transition into the orbital-ordered phase [20]. One puzzling issue is that for the former compounds, it is claimed that the role of the glassy phase (“electron glass”) is important in slow dynamics, whereas for the latter compound, no glassy phase is assumed and only the interfacial energy is taken into account for the slow dynamics upon the phase transition. It is important to determine whether the slow dynamics of these two different series of compounds share a common origin. It should also be pointed out that supercooling

behavior in various phase transitions of solids has been reported [21–23].

For the nucleation-growth behavior, the interfacial energy between two phases is taken into account, but the elastic energy of both phases is not. Nevertheless, the elastic energy of solid states is usually not negligible, and it is important to determine how it affects the nucleation-growth behavior. In relation to this issue, the crystal structure of $\text{BaV}_{10}\text{O}_{15}$ changes from orthorhombic (space group $Cmce$) to orthorhombic ($Pbca$) with orbital ordering [24,25]; thus, no twin structures or variants appear in the LT phase. This is an exceptional situation, and in many compounds, twin structures appear upon transition from the HT phase to the LT phase because of the lowering of crystal symmetry. The existence of such twin structures may affect the nucleation-growth process in solid states, and it is desirable to compare the slow dynamics in $\text{BaV}_{10}\text{O}_{15}$ and those in other compounds that exhibit a similar orbital ordering with twin structures.

In the present study, we investigate the slow dynamics of $\text{BaV}_{13}\text{O}_{18}$, which has a quasitriangular lattice of V ions and exhibits V trimerization below 70 K [26–30], similar to that of $\text{BaV}_{10}\text{O}_{15}$. This V trimerization is likely caused by the bond formation of the d_{xy} , d_{yz} , and d_{zx} orbitals at each edge of the triangle, which was experimentally confirmed for $\text{BaV}_{10}\text{O}_{15}$ [31]. Unlike in the case of $\text{BaV}_{10}\text{O}_{15}$, however, the crystal symmetry of $\text{BaV}_{13}\text{O}_{18}$ in the LT phase (triclinic) is lower than that in the HT phase (trigonal); thus, twin structures should appear in the LT phase. Furthermore, it is known that there is another phase, the intermediate-temperature (IT) phase, between the LT phase with V trimerization and the HT phase, which is characterized by a weak superstructure possibly caused by charge ordering [26], and the transition temperature between the LT phase and the IT phase can be increased by substituting Sr for Ba [27,29]. Thus, by investigating the dynamics of the phase transition in $\text{Ba}_{1-x}\text{Sr}_x\text{V}_{13}\text{O}_{18}$, we can determine how the twin structures affect the dynamics of the nucleation-growth process in solids

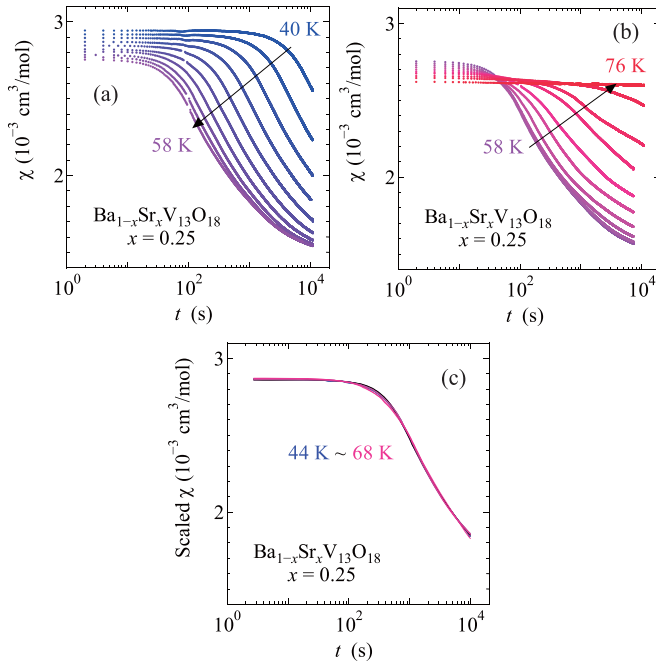


FIG. 1. (a) and (b) Time t dependence of the magnetic susceptibility χ for $\text{Ba}_{1-x}\text{Sr}_x\text{V}_{13}\text{O}_{18}$ with $x = 0.25$ measured every 2 K (a) between 40 and 58 K and (b) 58 and 76 K. (c) Results of the scaling with the relation $a\chi(t/c) + b = \chi_{48\text{K}}(t)$ for $\text{Ba}_{1-x}\text{Sr}_x\text{V}_{13}\text{O}_{18}$ with $x = 0.25$ between 44 and 68 K.

and also how various parameters in the dynamics change with the transition temperature.

II. EXPERIMENT

We grew single crystals of $\text{Ba}_{1-x}\text{Sr}_x\text{V}_{13}\text{O}_{18}$ as described in Ref. [28]. The magnetic susceptibility of the crystals was measured using a superconducting quantum interference device magnetometer. Since there is almost no anisotropy in the magnetic susceptibility in this series of compounds [29], we measured it for crystals with unknown axis directions. The strain in a crystal was measured using a strain gauge technique along a specific direction of the crystal, the orientation of which was determined using a Laue method.

To measure the time dependence of the magnetic susceptibility and strain associated with the transition from the IT phase to the LT phase in $\text{Ba}_{1-x}\text{Sr}_x\text{V}_{13}\text{O}_{18}$, we have to reduce the temperature of the crystal to the target temperature as rapidly as possible so that the sample does not undergo a transition to the LT phase before the start of measurement. For the strain measurement, a heater is attached to the sample, in addition to the heater for the heat bath, and rapid cooling to the target temperature was achieved by turning on and off the heater attached to the sample. For the magnetic susceptibility measurement, the sample was cooled at the highest cooling rate of the magnetometer (50 K/min).

III. RESULTS: MAGNETIC SUSCEPTIBILITY

Figures 1(a) and 1(b) show the magnetic susceptibility χ as a function of time t on a log scale at various temperatures T

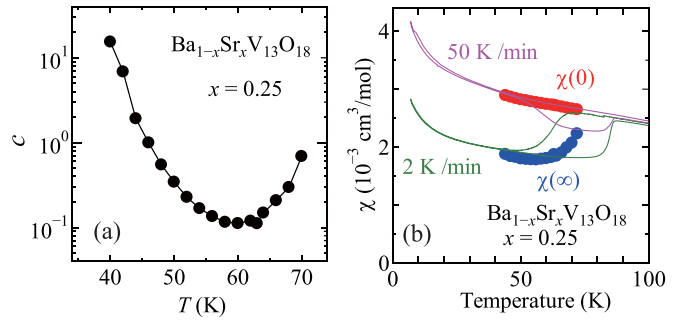


FIG. 2. (a) Temperature T dependence of c obtained by the scaling analysis of the magnetic susceptibility for $\text{Ba}_{1-x}\text{Sr}_x\text{V}_{13}\text{O}_{18}$ with $x = 0.25$ shown in Fig. 1(c). (b) T dependence of the magnetic susceptibility χ for $\text{Ba}_{1-x}\text{Sr}_x\text{V}_{13}\text{O}_{18}$ with $x = 0.25$ measured at cooling and heating rates of 50 and 2 K/min (solid lines), together with $\chi(0)$ and $\chi(\infty)$ obtained by the scaling analysis with Eq. (1) (solid circles).

for $\text{Ba}_{1-x}\text{Sr}_x\text{V}_{13}\text{O}_{18}$ with $x = 0.25$. As can be seen, χ exhibits a clear t dependence; χ is nearly constant for a while, it begins to decrease at a certain time, and it reaches saturation after more time passes. The time at which χ begins to decrease, called the transformation time, is found to decrease with increasing temperature T from 40 to 58 K but increases from 58 to 76 K. Such a t dependence of χ and a T dependence of the transformation time for χ are similar to those for $\text{BaV}_{10}\text{O}_{15}$ [20], although the decrease in χ with t for $\text{BaV}_{10}\text{O}_{18}$ is more gradual than that for $\text{BaV}_{10}\text{O}_{15}$.

Before discussing in detail the t dependence of χ , we first conduct a scaling analysis of $\chi(t)$ at various T values. Namely, we choose $\chi(t)$ at 48 K [$\chi_{48\text{K}}(t)$] as reference data and evaluate a , b , and c at each T in such a way that $a\chi(t/c) + b$ overlaps with $\chi_{48\text{K}}(t)$. Here, c corresponds to the scaling parameter for the t axis, whereas a and b are introduced because the initial and final values of $\chi(t)$ [$\chi(0)$ and $\chi(\infty)$] depend on T . The results of the scaling analysis for the data between $T = 44$ and 68 K are shown in Fig. 1(c).

The T dependence of the parameters determined by the scaling analysis is shown in Fig. 2. Here, instead of a and b , we plot $\chi(0)$ and $\chi(\infty)$, which are related to a and b as

$$a\chi(0) + b = \chi_{48\text{K}}(0 \text{ s}), \quad a\chi(\infty) + b = \chi_{48\text{K}}(10^4 \text{ s}). \quad (1)$$

This means that $\chi(0)$ and $\chi(\infty)$ correspond to the hypothetical values of $\chi(t)$ at $t = 0$ s and $t = \infty$, respectively, at each T . On the other hand, c corresponds to the relative transformation time at each T . As shown in Fig. 2(a), c as a function of T exhibits U-shaped behavior. $\chi(0)$ and $\chi(\infty)$ are plotted together with $\chi(T)$ measured at cooling and heating rates of 50 and 2 K/min in Fig. 2(b). $\chi(0)$ at various T values almost follows $\chi(T)$ measured at 50 K/min, whereas $\chi(\infty)$ almost follows $\chi(T)$ measured at 2 K/min.

Next, let us discuss the t dependence of χ more quantitatively. First, we assume that the transformed volume in the nucleation-growth process can be described by the KJMA model [10–13], which takes into account nucleation, the growth of the nuclei, and the impingement of the grown

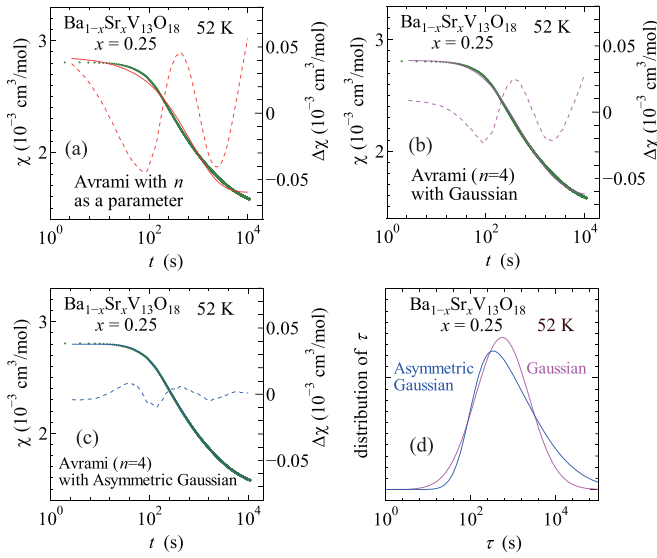


FIG. 3. (a)–(c) Temperature T dependence of the magnetic susceptibility for $\text{Ba}_{1-x}\text{Sr}_x\text{V}_{13}\text{O}_{18}$ with $x = 0.25$ at 52 K (dots, left axis) for the fitting using (a) a KJMA formula [Eq. (2)], (b) a KJMA formula with a distribution of τ by a Gaussian [Eqs. (3) and (4)], and (c) a KJMA formula with a distribution of τ by an asymmetric Gaussian (solid lined, left axis) and the difference between the experimental data and the fitting (dashed lines, right axis). (d) Distribution of the transformation time τ by a Gaussian and an asymmetric Gaussian for the fittings in (b) and (c), respectively.

nuclei. On the basis of this model, $\chi(t)$ is given by

$$\chi(t) = [\chi(0) - \chi(\infty)] \exp\left\{-\left(\frac{t}{\tau}\right)^n\right\} + \chi(\infty), \quad (2)$$

where τ is the transformation time and n is the Avrami exponent, which is theoretically given by the spatial dimension + 1. Figure 3(a) shows the fitting of $\chi(t)$ at 52 K using Eq. (2). However, n obtained from the fitting is ~ 0.75 , which is an unrealistic value since it should be the spatial dimension + 1, and the result of the fitting is still unsatisfactory, judging from the difference between the experimental result and the fitting shown by the dashed line in Fig. 3(a).

As a more realistic model, we consider the distribution of the transformation time τ . Namely, $\chi(t)$ is given by Eq. (2) but with a distribution of $\ln \tau = x$ as follows:

$$\chi(t) = \int_0^\infty \left[[\chi(0) - \chi(\infty)] \exp\left\{-\left(\frac{t}{e^x}\right)^4\right\} \right] A(x) dx + \chi(\infty). \quad (3)$$

Here, as the distribution function for $\ln \tau = x$, we assume a Gaussian [32],

$$A(x) = \frac{1}{\gamma\sqrt{\pi}} \exp\left\{-\frac{(x-x_0)^2}{\gamma^2}\right\}. \quad (4)$$

For the fitting using Eqs. (3) and (4), the Avrami exponent n is fixed at 4, and the median of the transformation time, $x_0 = \ln \tau_0$, and the width of the distribution γ are estimated as the fitting parameters. Note that the number of parameters in the fitting using Eqs. (3) and (4) [χ_0 , γ , $\chi(0)$, and $\chi(\infty)$] is the same as that using Eq. (2) [τ , n , $\chi(0)$, and $\chi(\infty)$]. The

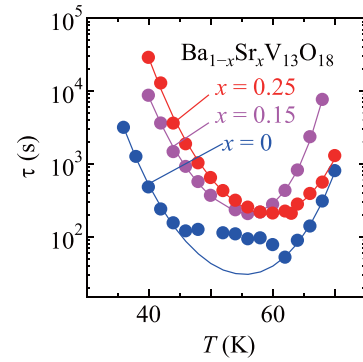


FIG. 4. Temperature T dependence of the transformation time τ for $\text{Ba}_{1-x}\text{Sr}_x\text{V}_{13}\text{O}_{18}$ with $x = 0, 0.15$, and 0.25 . The solid lines are the fitting curves using Eq. (5).

result of the fitting and the functional form of $A(x) = A(\ln \tau)$ are shown in Figs. 3(b) and 3(d), which show better agreement with the experimental result than the fitting using Eq. (2). We found that further better agreement between the fitting and the experimental result can be obtained by assuming an asymmetric Gaussian for $A(x)$, as shown in Figs. 3(c) and 3(d), although five fitting parameters are necessary. This is discussed in more detail, including the possible origin of the asymmetry, in Appendix A.

To discuss the T dependence of the transformation time τ with a distribution, we define τ at 52 K as the peak of the Gaussian obtained from the fitting using Eqs. (3) and (4). On the basis of this absolute value of τ at 52 K, together with the T dependence of the relative change in the transformation time c obtained from the scaling analysis, the T dependence of the transformation time τ can be obtained, as shown in Fig. 4, which is generally called a time-temperature-transformation (TTT) curve.

Note that there are other ways to estimate the T dependence of the transformation time τ without using the scaling analysis by fitting the t dependence of χ at each T using Eq. (3) either with a Gaussian given by Eq. (4) or an asymmetric Gaussian for $A(x)$ and defining τ as the peak of $A(x)$. This is discussed in Appendix B.

Let us next analyze the TTT curve. The TTT curve $\tau(T)$ obtained above was fitted by the formula for the nucleation and growth process [2,7]:

$$\tau = \tau_{\text{ph}} \exp\left(\frac{T_1}{T}\right) \exp\left(\frac{T_2^3}{(T_c - T)^2 T}\right), \quad (5)$$

where T_1 corresponds to the height of the energy barrier between the LT phase and the IT phase per atom, T_2 is determined by the interfacial energy between the LT phase and the IT phase, and T_c is a hypothetical transition temperature between the LT phase and the IT phase. The result of the fitting is shown by a solid line in Fig. 4. The obtained parameters for $\text{Ba}_{1-x}\text{Sr}_x\text{V}_{13}\text{O}_{18}$ with $x = 0.25$ are as follows: $T_1 = 923$ K, $T_2 = 116$ K, $T_c = 108$ K, and $\tau_{\text{ph}} = 7 \times 10^{-10}$ s.

We apply the same analysis procedure to $\text{Ba}_{1-x}\text{Sr}_x\text{V}_{13}\text{O}_{18}$ with $x = 0$ and $x = 0.15$, and the results are shown in Figs. 5–9. There are several issues on these results that have to be discussed. First, for $x = 0$, $\chi(0)$ is discernibly smaller than $\chi(T)$ measured at a cooling rate of 50 K/min between

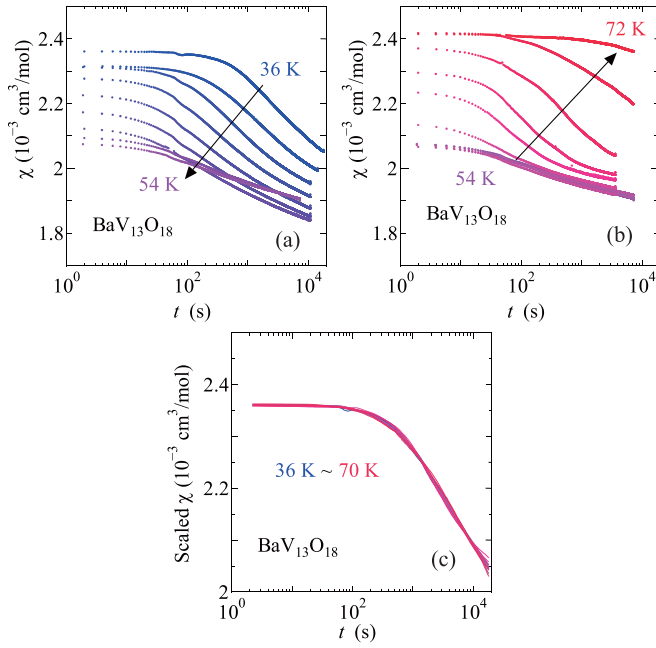


FIG. 5. (a) and (b) Time t dependence of the magnetic susceptibility χ for $\text{BaV}_{13}\text{O}_{18}$ measured every 2 K (a) between 36 and 54 K and (b) between 54 and 72 K. (c) Results of the scaling with the relation $a\chi(t/c) + b = \chi_{36\text{K}}(t)$ for $\text{BaV}_{13}\text{O}_{18}$ at T between 36 and 70 K.

45 and 65 K, as shown in Fig. 6(b). In this T range, the T dependence of the transformation time τ is flattened, as shown in Fig. 6(a). These results indicate that in this T range, part of the crystal has already undergone a transition to the LT phase before the start of the measurement because of the too short transformation time near the bottom of the TTT curve. Such a deviation of the TTT curve from a smooth U shape was reported for several compounds [17,18], where the TTT curve was interpreted as having two minima and the two minima were assigned to the nucleation- and growth-dominated regimes. We point out that in Eq. (5), $\exp(T_1/T)$ corresponds to the growth, whereas $\exp[T_2^3/(T_c - T)^2T]$ corresponds to the nucleation, but the product of the two does not produce two minima.

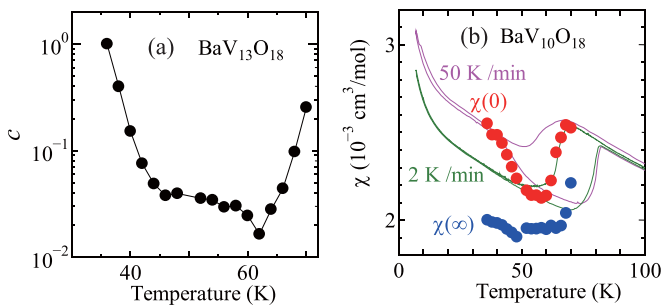


FIG. 6. (a) Temperature T dependence of c obtained from the scaling analysis of the magnetic susceptibility for $\text{BaV}_{13}\text{O}_{18}$ shown in Fig. 5(c). (b) T dependence of the magnetic susceptibility χ for $\text{BaV}_{13}\text{O}_{18}$ measured at cooling and heating rates of 50 and 2 K/min (solid lines), together with $\chi(0)$ and $\chi(\infty)$ obtained from the scaling analysis with Eq. (1) (solid circles).

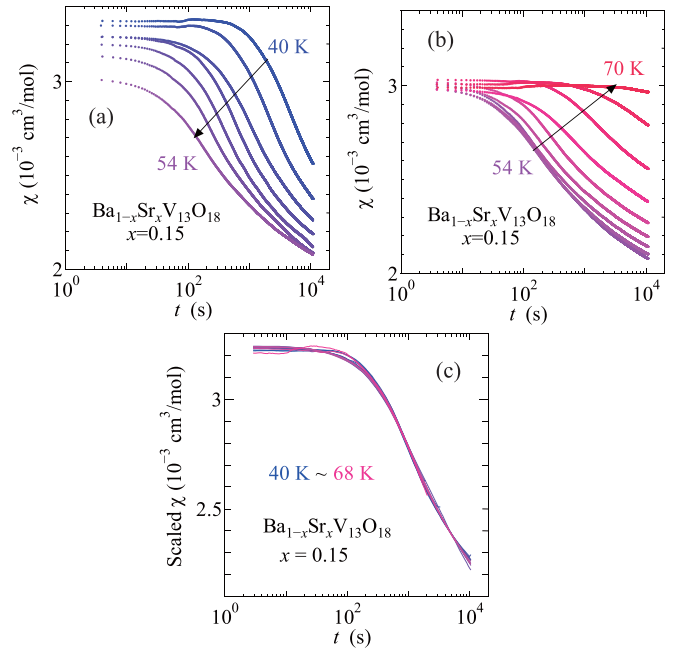


FIG. 7. (a) and (b) Time t dependence of the magnetic susceptibility χ for $\text{Ba}_{1-x}\text{Sr}_x\text{V}_{13}\text{O}_{18}$ with $x = 0.15$ measured every 2 K (a) between 40 and 54 K and (b) between 54 and 70 K. (c) Results of the scaling with the relation $a\chi(t/c) + b = \chi_{44\text{K}}(t)$ for $\text{Ba}_{1-x}\text{Sr}_x\text{V}_{13}\text{O}_{18}$ with $x = 0.25$ between 40 and 68 K.

Second, $\chi(\infty)$ for $x = 0$ and $x = 0.15$ becomes much lower than $\chi(T)$ measured at a cooling rate of 2 K/min, as shown in Figs. 6(b) and 8(b). This means that such a cooling rate during the measurement of the T dependence is not sufficiently low for the system to settle into a phase with lower free energy. Indeed, if we wait 10^4 s at 54 K, at which the TTT curve takes the minimum, and then measure the T dependence of χ for $x = 0.15$ [dashed line in Fig. 8(b)], $\chi(T)$ further decreases from that measured at the cooling rate of 2 K/min.

The transformation time for $x = 0$ and $x = 0.15$ obtained from the scaling analysis and the fitting of $\chi(t)$ at one

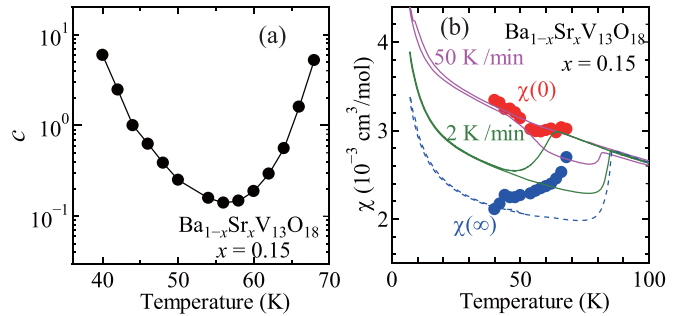


FIG. 8. (a) Temperature T dependence of c obtained from the scaling analysis of the magnetic susceptibility for $\text{Ba}_{1-x}\text{Sr}_x\text{V}_{13}\text{O}_{18}$ with $x = 0.15$ shown in Fig. 7(c). (b) T dependence of the magnetic susceptibility χ for $\text{Ba}_{1-x}\text{Sr}_x\text{V}_{13}\text{O}_{18}$ with $x = 0.15$ measured at cooling and heating rates of 50 and 2 K/min (solid lines), measured after waiting 10^4 s at 54 K (dashed line), and with $\chi(0)$ and $\chi(\infty)$ obtained from the scaling analysis with Eq. (1) (solid circles).

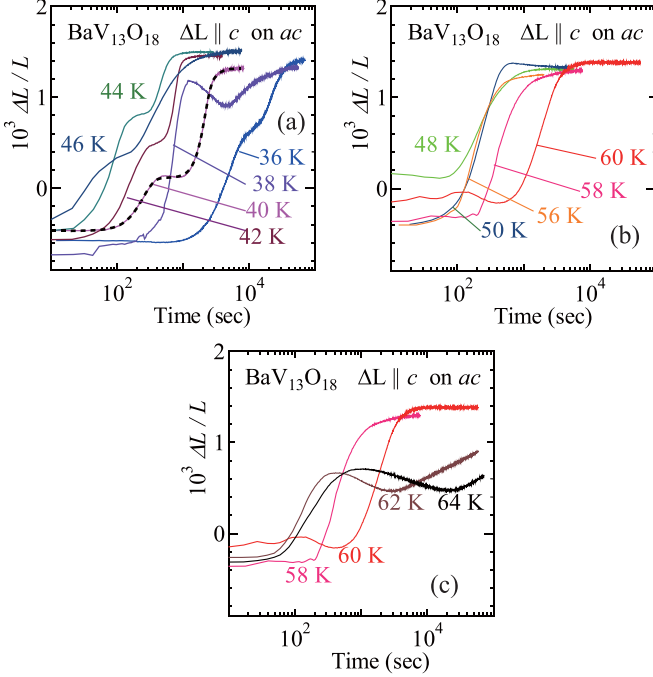


FIG. 9. (a)–(c) Time t dependence of the strain $\Delta L/L$ for $\text{BaV}_{13}\text{O}_{18}$ (a) between 36 and 46 K, (b) between 48 and 60 K, and (c) between 58 and 64 K. The zero value of $\Delta L/L$ corresponds to the value at 100 K.

temperature is plotted as a function of T in Fig. 4, together with that for $x = 0.25$. These TTT curves were fitted using Eq. (5), and the parameters obtained from the fitting for $x = 0, 0.15$, and 0.25 are summarized in Table I. It is found that T_1 , corresponding to the height of the energy barrier between the LT phase and the IT phase, increases with x . It is likely that this energy barrier is dominated by the coupling between the orbital degree of freedom of the V ion and the lattice distortion, and since the transition temperature of orbital ordering increases with x in $\text{Ba}_{1-x}\text{Sr}_x\text{V}_{13}\text{O}_{18}$, the magnitude of the coupling will also increase with x , consistent with the present experimental result. However, other parameters do not exhibit a systematic change with x .

IV. RESULTS: STRAIN

We also measured the t dependence of strain $\Delta L/L$ along the c axis on the ac plane for $\text{BaV}_{13}\text{O}_{18}$. As shown in Figs. 9(a)–9(c), the strain at each T exhibits clear t dependence. The time when $\Delta L/L$ begins to increase τ_0 becomes minimum at around 50–56 K, and with increasing or decreasing T from this T range, τ_0 increases similarly to the

TABLE I. Parameters obtained from the fitting of the TTT curves using Eq. (5).

x	T_1 (K)	T_2 (K)	T_c (K)	τ_{ph} (s)
0	685	114	106	4×10^{-9}
0.15	852	79	91	4×10^{-8}
0.25	923	116	108	7×10^{-10}

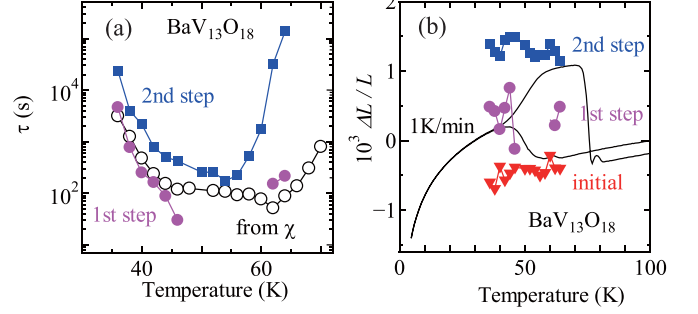


FIG. 10. (a) Temperature dependence of the transformation time τ for $\text{BaV}_{13}\text{O}_{18}$ obtained in the first and second steps in the t dependence of $\Delta L/L$ (purple circles and blue squares, respectively), together with τ estimated from the magnetic susceptibility (black open circles). (b) $\Delta L/L$ in the initial state (red triangles), first step (purple circles), and second step (approximately the final state, blue squares) obtained from the fitting of the t -dependent $\Delta L/L$ at each T , together with the T dependence of $\Delta L/L$ measured at cooling and heating rates of 1 K/min (solid lines).

magnetic susceptibility χ of the same compound [Figs. 5(a) and 5(b)]. However, the t dependence of $\Delta L/L$ often exhibits two-step behavior, and the t dependence of each step in $\Delta L/L$ is sharper than that of χ .

The t dependence of $\Delta L/L$ is fitted by a sum of more than one KJMA term given by Eq. (2). Namely,

$$\Delta L/L = a_0 + \sum_i a_i \exp \left\{ - \left(\frac{t}{\tau_i} \right)^{n_i} \right\}. \quad (6)$$

Here, $\Delta L/L$ as a function of t at several T values (38 K, for example) decreases in the first step. In such a case, we assume the sum of three KJMA terms for which the sign of a_i for the second term is different (positive in this case) from that of the other a_i to reproduce the decrease in the first step. In other cases, we assume two KJMA terms or a single KJMA term depending on the existence or absence of the two steps in the t dependence of $\Delta L/L$ at each T . A typical example of the fitting of the experimental data is shown for the data at 40 K by a dashed line in Fig. 9(a). Figure 10(a) shows the transformation time τ for the first and second steps as a function of T , together with τ estimated from the magnetic susceptibility (Fig. 4). As can be seen, the transformation time for the first step seems consistent with that estimated from the magnetic susceptibility.

Figure 10(b) shows the value of $\Delta L/L$ in the initial state (red triangles), first step (purple circles), and second step (approximately the final state, blue squares) for the t dependence of $\Delta L/L$ at each T , together with the T dependence of $\Delta L/L$ measured at cooling and heating rates of 1 K/min. As can be seen, the T dependence of $\Delta L/L$ at cooling and heating rates of 1 K/min does not follow the values in the second step of the t dependence, indicating that the cooling rate of 1 K/min is still too high for the system to settle into the LT phase. Furthermore, the value in the first step does not exhibit a systematic change but instead changes rather randomly with T , and this is already seen in the t dependence of $\Delta L/L$ shown in Figs. 9(a)–9(c). This indicates that the two steps in the t

dependence of $\Delta L/L$ are not caused by the contribution of two parts in the crystal with fixed volumes.

V. DISCUSSION

We first discuss the similarities and differences in the dynamics of the phase transition in $\text{Ba}_{1-x}\text{Sr}_x\text{V}_{13}\text{O}_{18}$ and $\text{BaV}_{10}\text{O}_{15}$, which was previously reported [20]. In both compounds, magnetic susceptibility χ and strain $\Delta L/L$ exhibit t dependence, and the transformation time at each T estimated from the t dependence of χ and $\Delta L/L$ exhibits a clear U shape as a function of T , which is consistent with the nucleation-growth process. On the other hand, the t dependence of both χ and $\Delta L/L$ obeys the KJMA formula with $n = 3-4$ for $\text{BaV}_{10}\text{O}_{15}$ [20]. However, in the case of $\text{Ba}_{1-x}\text{Sr}_x\text{V}_{13}\text{O}_{18}$, there is a distribution of the transformation time for the dynamics of χ , and there is two-step behavior in the t dependence of $\Delta L/L$, meaning that there are at least two different transformation times.

One of the different characteristics between the phase transition in $\text{Ba}_{1-x}\text{Sr}_x\text{V}_{13}\text{O}_{18}$ and that in $\text{BaV}_{10}\text{O}_{15}$ is the existence or absence of twin structures upon the phase transition. In the case of $\text{BaV}_{10}\text{O}_{15}$, the space group changes from $Cmce$ to $Pbca$ [24,25], both of which belong to the orthorhombic crystal system; thus, no twin structures appear after the phase transition. On the other hand, in $\text{Ba}_{1-x}\text{Sr}_x\text{V}_{13}\text{O}_{18}$, the space group changes from $R\bar{3}$ to $P\bar{1}$ [26], namely, from trigonal (HT) to triclinic (LT), with the phase transition, and thus, twin structures appear after the phase transition.

The dominant parameter in the nucleation-growth process is the interfacial energy between the two phases, whereas the elastic energy as a bulk property is not taken into account in the derivation of the KJMA formula or in the analysis based on the formula. However, in the case of structural phase transitions in solid states, such elastic energy may affect their dynamics. We point out that the existence of twin structures causes a spatial distribution of the strain tensor in the crystal, which may result in the distribution of the transformation time. More specifically, the formation of a variant elongating in one direction may reduce the elastic energy of nearby nuclei elongating in the same direction compared with those elongating in a different direction. This can cause different transformation times for different nuclei and can explain the distribution of the transformation time in $\text{Ba}_{1-x}\text{Sr}_x\text{V}_{13}\text{O}_{18}$.

Regarding the result of the strain measurement, we point out that the attachment of the strain gauge itself will affect twin structures. Namely, since the strain gauge is composed of a metal foil on the plastic substrate, a large thermal contraction of the plastic substrate causes compressive strain on the surface to which the strain gauge is attached, and it induces a selection of specific domains (variants) of twin structures [33]. In the present case, the transition from a trigonal to a triclinic phase allows six variants corresponding to the permutation of three primitive vectors of the triclinic phase, but two variants will be preferentially selected if a strain gauge is attached to the (100) plane of the crystal [34]. One possibility is that the two-step behavior in the t dependence of the strain arises from two such variants, probably with large volumes selected by the attachment of a strain gauge. The experimental result that

the value of the first step in $\Delta L/L$, which corresponds to the volume fraction of one phase, does not exhibit a systematic change with T , as shown in Figs. 9 and 10, may be caused by the fact that such selection of variants strongly depends on how the sample experiences rapid cooling, and thus, the volume fraction can be different for the measurement at different temperatures. On the other hand, there is no such process of the selection for variants in the magnetic susceptibility measurement, and thus, all six kinds of variants with small volumes are present, resulting in the Gaussian-type distribution of the transformation time.

We also discuss the x dependence of various parameters obtained from the fitting of the TTT curve shown in Table I. It is found that T_1 increases with x , indicating that the height of the energy barrier between the LT phase and the IT phase increases with x . On the other hand, T_2 and T_c do not change systematically with x . Indeed, as discussed in Appendix B, the fitting of the T dependence of the transformation time τ (TTT curve) obtained using the different methods gives different values of T_1 , T_2 , and T_c . We found that, although the x dependence of T_1 does not change qualitatively with the different methods of estimating τ , T_2 and T_c change qualitatively. In other words, the accuracy of the present experiment may not be sufficient to discuss the difference in dynamics for different x values in $\text{Ba}_{1-x}\text{Sr}_x\text{V}_{13}\text{O}_{18}$.

VI. CONCLUSION

We studied the slow dynamics of orbital ordering accompanied by V trimerization in $\text{Ba}_{1-x}\text{Sr}_x\text{V}_{13}\text{O}_{18}$ consisting of quasitriangular lattices of V ions. We found that the magnetic susceptibility of this series of compounds exhibits a clear time t dependence. However, the t dependence cannot be fitted by a simple KJMA formula, a typical formula for nucleation-growth processes; the distribution of the transformation time τ has to be taken into account. The temperature T dependence of τ exhibits a U shape with T as the x axis, consistent with a model of phase transitions dominated by the nucleation-growth process. We also found that the t dependence of strain for $\text{Ba}_{1-x}\text{Sr}_x\text{V}_{13}\text{O}_{18}$ exhibits two-step behavior, indicating that there are two different transformation times. These results are in contrast to those for $\text{BaV}_{10}\text{O}_{15}$, which consists of a quasitriangular lattice of V ions and exhibits orbital ordering with V trimerization similar to $\text{Ba}_{1-x}\text{Sr}_x\text{V}_{13}\text{O}_{18}$ but exhibits slow dynamics following a simple KJMA formula with a single τ . This difference can be attributed to the existence ($\text{Ba}_{1-x}\text{Sr}_x\text{V}_{13}\text{O}_{18}$) or absence ($\text{BaV}_{10}\text{O}_{15}$) of twin structures in the LT phase associated with the phase transition. Namely, the existence of twin structures could lead to a spatial distribution of strain, which could affect the dynamics of the phase transition through the elastic energy of the nuclei.

ACKNOWLEDGMENT

This work was supported by JSPS KAKENHI Grant No. 19H01853.

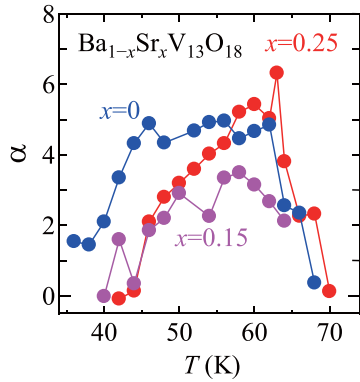


FIG. 11. T dependence of α in the asymmetric Gaussian, corresponding to its asymmetry, for $x = 0, 0.15$, and 0.25 .

APPENDIX A: DISTRIBUTION OF THE TRANSFORMATION TIME τ BY AN ASYMMETRIC GAUSSIAN

We consider a model in which $\chi(t)$ is given by Eq. (2) with a distribution of $\ln \tau = x$ by an asymmetric Gaussian. An asymmetric Gaussian, or a skew normal distribution, is given by

$$f(x) = \frac{1}{\pi} \exp\left(-\frac{x^2}{2}\right) \int_{-\infty}^{\alpha x} \exp\left(-\frac{t^2}{2}\right) dt. \quad (\text{A1})$$

Note that $f(x)$ with $\alpha = 0$ reduces to a normal Gaussian, and thus, α corresponds to the magnitude of asymmetry.

Using this $f(x)$, we fit the time dependence of magnetic susceptibility $\chi(t)$ from Eq. (3) with $A(x)$ as

$$A(x) = \frac{\sqrt{2}}{\gamma} f\left(\frac{\sqrt{2}(x - x_0)}{\gamma}\right). \quad (\text{A2})$$

Note that $x = \ln \tau$ and n (Avrami exponent) was fixed to 4 in the fitting. Thus, x_0 , γ , α , $\chi(0)$, and $\chi(\infty)$ are the fitting parameters.

An example of the fitting using Eqs. (3), (A1), and (A2) is shown in Fig. 3(c), and the functional form of $\sqrt{2}/\gamma \times f[\sqrt{2}(x - x_0)/\gamma]$ with $x = \ln \tau$ is shown in Fig. 3(d). As can be seen in Fig. 3(d), the slope is steeper on the lower side of the peak of $f[\sqrt{2}(x - x_0)/\gamma]$ because of positive α .

One of the results that makes this model likely is the T dependence of α shown in Fig. 11. As described above, α corresponds to the magnitude of asymmetry, and positive α means that the lower side of the peak is steeper. As can be seen in Fig. 11, α increases in the intermediate T range, where τ decreases, as shown in Fig. 4, and in particular, α is large when $x = 0$ between 40 and 60 K, where τ deviates from the smooth curve given by Eq. (5). These results indicate that the asymmetry in the distribution of τ arises from the fact that, even with a symmetric distribution of τ in the beginning, part of the crystal where τ is relatively small has already undergone the phase transition before the start of the measurement and does not contribute to the time dependence of χ .

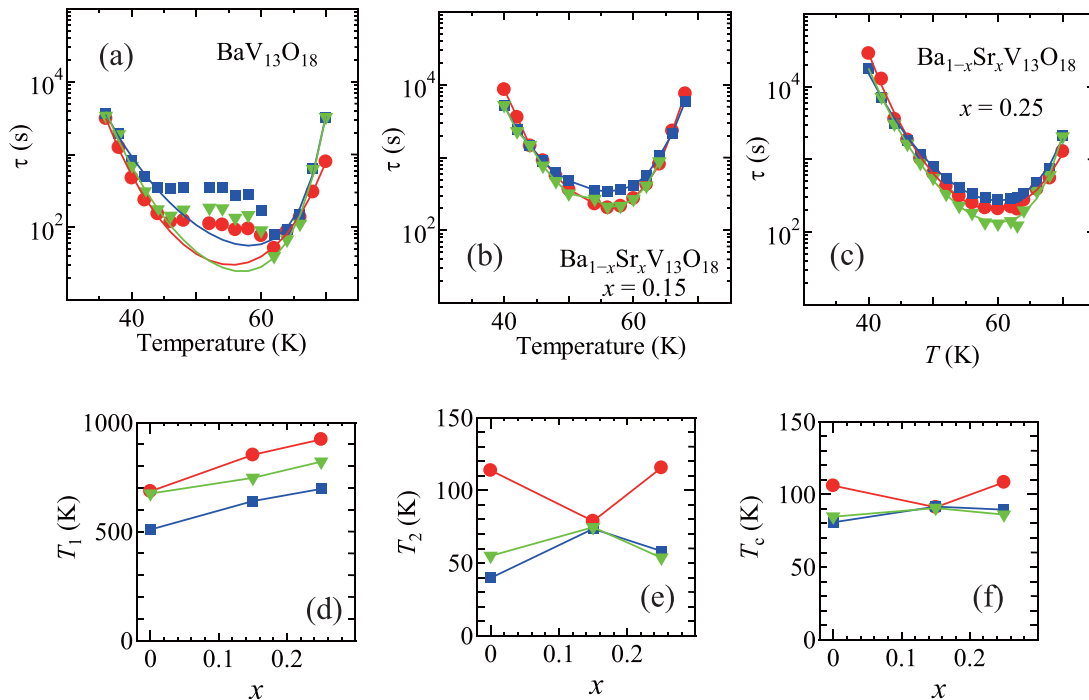


FIG. 12. (a)–(c) T dependence of the transformation time τ (TTT curve) obtained from the scaling analysis (red circles), that obtained from the fitting of $\chi(T)$ using the KJMA formula considering a distribution of τ with a Gaussian (blue squares), and that obtained from the KJMA formula considering a distribution of τ with an asymmetric Gaussian (green triangles) for $x = 0, 0.15$, and 0.25 , respectively. Solid lines are the fittings using Eq. (5). (d)–(f) x dependence of T_1 , T_2 , and T_c estimated from the fitting of the TTT curves using Eq. (5) obtained with the three different methods in (a)–(c). Symbols in (d)–(f) correspond to those in (a)–(c).

APPENDIX B: TRANSFORMATION TIME τ ESTIMATED USING VARIOUS METHODS

In the main text, the transformation time τ in the t dependence of magnetic susceptibility χ was estimated by obtaining relative changes in τ with T using the scaling analysis of $\chi(t)$, together with the absolute value of τ at one T estimated by the fitting of $\chi(t)$ using the KJMA formula considering a Gauss distribution of τ . On the other hand, we can obtain τ by simply fitting $\chi(t)$ using the KJMA formula and a specific distribution function of τ at all T values. Figures 12(a)–12(c) show the T dependences of τ obtained from the scaling analysis (the same as that in the main text, red

circles), that obtained from the fitting of $\chi(t)$ using the KJMA formula considering a distribution of τ with a Gaussian (blue squares), and that obtained from the fitting of $\chi(t)$ using the KJMA formula considering a distribution of τ with an asymmetric Gaussian (green triangles) for $x = 0, 0.15,$ and $0.25,$ respectively.

Figures 12(d)–12(f) show the x dependence of $T_1, T_2,$ and T_c estimated from the fitting of the TTT curve obtained using the three different methods described above. Although we observed that the x dependence of T_1 , that is, its monotonic increase with x , does not change for the three different estimates of τ , the x dependence of T_2 and T_c strongly depends on how τ is estimated.

- [1] E. Coleman, Crystallization of Fe, Co and Ni based metallic glasses, *Mater. Sci. Eng.* **23**, 161 (1976).
- [2] D. R. Uhlmann, Glass formation, *J. Non-Cryst. Solids* **25**, 42 (1977).
- [3] M. G. Scott, The crystallization kinetics of Fe-Ni based metallic glasses, *J. Mater. Sci.* **13**, 291 (1978).
- [4] S. Ranganathan and M. V. Heimendahl, The three activation energies with isothermal transformations: Applications to metallic glasses, *J. Mater. Sci.* **16**, 2401 (1981).
- [5] D. M. Herlach, Non-equilibrium solidification of undercooled metallic melts, *Mater. Sci. Eng., R* **12**, 177 (1994).
- [6] Y. J. Kim, R. Busch, W. L. Johnson, A. J. Rulison, and W. K. Rhim, Experimental determination of a time-temperature transformation diagram of the undercooled $\text{Zr}_{41.2}\text{Ti}_{13.8}\text{Cu}_{12.5}\text{Ni}_{10.0}\text{Be}_{22.5}$ alloy using the containerless electrostatic levitation processing technique, *Appl. Phys. Lett.* **68**, 1057 (1996).
- [7] J. F. Löffler, J. Schroers, and W. L. Johnson, Time-temperature-transformation diagram and microstructures of bulk glass forming $\text{Pd}_{40}\text{Cu}_{30}\text{Ni}_{10}\text{P}_{20}$, *Appl. Phys. Lett.* **77**, 681 (2000).
- [8] J. Orava, A. L. Greer, B. Gholipour, D. W. Hewak, and C. E. Smith, Characterization of supercooled liquid $\text{Ge}_2\text{Sb}_2\text{Te}_5$ and its crystallization by ultrafast-heating calorimetry, *Nat. Mater.* **11**, 279 (2012).
- [9] Y. Sutou, T. Kamada, M. Sumiya, Y. Saito, and J. Koike, Crystallization process and thermal stability of $\text{Ge}_1\text{Cu}_2\text{Te}_3$ amorphous thin films for use as phase change materials, *Acta Mater.* **60**, 872 (2012).
- [10] A. N. Kolmogorov, Statistical theory of nucleation processes, *Bull. Acad. Sci. USSR, Math. Ser.* **3**, 355 (1937).
- [11] W. A. Johnson and P. A. Mehl, Reaction kinetics in processes of nucleation and growth, *Trans. Am. Inst. Min., Metall. Eng.* **135**, 416 (1939).
- [12] M. Avrami, Kinetics of phase change. I. General theory, *J. Chem. Phys.* **7**, 1103 (1939).
- [13] J. Christian, *The Theory of Transformations in Metals and Alloys* (Pergamon, Oxford, 2002).
- [14] Y. Yamada, N. Hamaya, J. D. Axe, and S. M. Shapiro, Nucleation, Growth, and Scaling in a Pressure-Induced First-Order Phase Transformation: RbI, *Phys. Rev. Lett.* **53**, 1665 (1984).
- [15] H. Abe, M. Ishibashi, K. Ohshima, T. Suzuki, M. Wuttig, and K. Kakurai, Kinetics of the martensitic transition in In-Tl alloys, *Phys. Rev. B* **50**, 9020 (1994).
- [16] F. Kagawa, T. Sato, K. Miyagawa, K. Kanoda, Y. Tokura, K. Kobayashi, R. Kumai, and Y. Murakami, Charge-cluster glass in an organic conductor, *Nat. Phys.* **9**, 419 (2013).
- [17] S. Sasaki, K. Hashimoto, R. Kobayashi, K. Itoh, S. Iguchi, Y. Nishio, Y. Ikemoto, T. Moriwaki, N. Yoneyama, M. Watanabe, A. Ueda, H. Mori, K. Kobayashi, R. Kumai, Y. Murakami, J. Müller, and T. Sasaki, Crystallization and vitrification of electrons in a glass-forming charge liquid, *Science* **357**, 1381 (2017).
- [18] T. Sato, K. Miyagawa, and K. Kanoda, Electronic crystal growth, *Science* **357**, 1378 (2017).
- [19] T. Sato, K. Kitai, K. Miyagawa, M. Tamura, A. Ueda, H. Mori, and K. Kanoda, Strange metal from a frustration-driven charge order instability, *Nat. Mater.* **18**, 229 (2019).
- [20] T. Katsufuji, T. Kajita, S. Yano, Y. Katayama, and K. Ueno, Nucleation and growth of orbital ordering, *Nat. Commun.* **11**, 2324 (2020).
- [21] H. Oike, A. Kikkawa, N. Kanazawa, Y. Taguchi, M. Kawasaki, Y. Tokura, and F. Kagawa, Interplay between topological and thermodynamic stability in a metastable magnetic skyrmion lattice, *Nat. Phys.* **12**, 62 (2016).
- [22] H. Oike, M. Kamitani, Y. Tokura, and F. Kagawa, Kinetic approach to superconductivity hidden behind a competing order, *Sci. Adv.* **4**, eaau3489 (2018).
- [23] K. Matsuura, H. Oike, V. Kocsis, T. Sato, Y. Tomioka, Y. Kaneko, M. Nakamura, Y. Taguchi, M. Kawasaki, Y. Tokura, and F. Kagawa, Kinetic pathway facilitated by a phase competition to achieve a metastable electronic phase, *Phys. Rev. B* **103**, L041106 (2021).
- [24] C. A. Bridges and J. E. Greedan, Phase transitions and electrical transport in the mixed-valence $\text{V}^{2+}/\text{V}^{3+}$ oxide $\text{BaV}_{10}\text{O}_{15}$, *J. Solid State Chem.* **177**, 1098 (2004).
- [25] T. Kajita, T. Kanzaki, T. Suzuki, J. E. Kim, K. Kato, M. Takata, and T. Katsufuji, Opening of a charge gap with V trimerization in $\text{BaV}_{10}\text{O}_{15}$, *Phys. Rev. B* **81**, 060405(R) (2010).
- [26] M. Ikeda, Y. Nagamine, S. Mori, J. E. Kim, K. Kato, M. Takata, and T. Katsufuji, Phase transitions and the role of vanadium t_{2g} states in $\text{AV}_{13}\text{O}_{18}$ ($A = \text{Sr}, \text{Ba}$), *Phys. Rev. B* **82**, 104415 (2010).
- [27] M. Ikeda, T. Okuda, K. Kato, M. Takata, and T. Katsufuji, Competition between vanadium tetramerization and trimerization in $\text{Ba}_{1-x}\text{Sr}_x\text{V}_{13}\text{O}_{18}$, *Phys. Rev. B* **83**, 134417 (2011).

- [28] T. Kanzaki, J. Fujioka, Y. Tokura, H. Kuwahara, and T. Katsufuji, Anomalous metallic ground state in $\text{BaV}_{13}\text{O}_{18}$, *Phys. Rev. B* **89**, 140401(R) (2014).
- [29] T. Kajita, Y. Obata, Y. Kakesu, Y. Imai, Y. Shmizu, M. Itoh, H. Kuwahara, and T. Katsufuji, Trimerization and orbital ordering in $\text{Ba}_{1-x}\text{Sr}_x\text{V}_{13}\text{O}_{18}$, *Phys. Rev. B* **96**, 245126 (2017).
- [30] K. Funahashi, Y. Kakesu, T. Kajita, Y. Obata, Y. Katayama, K. Ueno, T. Suzuki, J. G. Checkelsky, and T. Katsufuji, Magnetotransport properties of the orbital-ordered state of $\text{Ba}_{1-x}\text{Sr}_x\text{V}_{13}\text{O}_{18}$, *J. Phys. Soc. Jpn.* **88**, 024708 (2019).
- [31] K. Takubo, T. Kanzaki, Y. Yamasaki, H. Nakao, Y. Murakami, T. Oguchi, and T. Katsufuji, Orbital states of V trimers in $\text{BaV}_{10}\text{O}_{15}$ detected by resonant x-ray scattering, *Phys. Rev. B* **86**, 085141 (2012).
- [32] According to Eq. (5), $\ln(\tau)$ is given by the sum of T_1/T , $T_2^3/(T_c - T)^2T$, and a constant. Thus, if a distribution of one of the parameters, for example, T_1 , is dominant and has a Gaussian distribution, $\ln(\tau)$ also has a Gaussian distribution, but if this is not the case, $\ln(\tau)$ will have a distribution different from a Gaussian.
- [33] T. Katsufuji, T. Suzuki, H. Takei, M. Shingu, K. Kato, K. Osaka, M. Takata, H. Sagayama, and T.-H. Arima, Structural and magnetic properties of spinel FeV_2O_4 with two ions having orbital degrees of freedom, *J. Phys. Soc. Jpn.* **77**, 053708 (2008).
- [34] See Supplemental Material at <http://link.aps.org/supplemental/10.1103/PhysRevB.106.045124> for a discussion of the calculation of strain after the phase transition and how the strain gauge attached to the (100) plane selects specific variants.